Transactions of the SMiRT 27
Yokohama, Japan, March 3-8, 2024
Division VII

RISK-INFORMED DESIGN OF A SEISMIC ISOLATION SYSTEM FOR ADVANCED NUCLEAR POWER PLANTS

Ching-Ching Yu[1], Benjamin M. Carmichael[2], Jason P. Redd[3], Brandon M. Chisholm[4], Mark W. Peres[5], Brian I. Song[6], Matthew Denman[7], Chandrakanth Bolisetti[8], and Andrew S. Whittaker[9]

[1] Former Postdoctoral Associate, University at Buffalo, Buffalo, NY (cyu23@buffalo.edu)
[2] Business Development Manager, Research and Development, Southern Company, Birmingham, AL
[3] Project Manager, Southern Nuclear Services, Birmingham, AL
[4] Advanced Nuclear R&D Engineer, Research and Development, Southern Company, Birmingham, AL
[5] President, Peres Engineering, Columbia, SC
[6] Senior Manager, Civil Structures, Kairos Power, Alameda, CA
[7] Distinguished Engineer, Kairos Power, Albuquerque, NM
[8] Senior Scientist, Risk Phenomena Modeling, Idaho National Laboratory, Idaho Falls, ID
[9] SUNY Distinguished Professor, University at Buffalo, Buffalo, NY

ABSTRACT

The US Department of Energy funded the development of a topical report on the seismic isolation of advanced nuclear power plants. The report, also available as Yu *et al*. (2023), includes a pathway to achieve a user-specified risk target for an isolation system, and that is the focus of this paper. A generic advanced reactor building, sited at Clinch River, TN, is used to illustrate the risk-informed approach. Two soil profiles, and seven 2D and 3D isolation systems with a range of dynamic properties, are considered in the report, to achieve different target performance goals. The expected performance of the isolation system is unrestricted horizontal displacement under earthquake shaking. Results for one soil profile and three isolation systems are presented in the paper.

INTRODUCTION

Seismic isolation systems can be installed below the basemat and above the foundation of an advanced nuclear reactor building to reduce accelerations and deformations on structures, systems, and components (SSCs) in the superstructure generated by earthquake shaking. A seismic isolation system, composed of isolators and damping elements and can be treated as an SSC for the purpose of analysis and design. The required performance of the isolation system is unrestricted horizontal displacement sufficient to achieve a target performance goal (TPG). To protect the SSCs in the isolated reactor building, the TPG assigned to the isolation system should be generally equal to or smaller than that for the SSCs. (For example, if the highest SDC assigned to the SSCs in the isolated reactor building is 3, namely, a TPG of 1×10^{-4}, the TPG assigned to the isolation system should be $\leq 1 \times 10^{-4}$.)

Yu *et al.* (2023) provides a risk-based process to establish the median displacement capacity of an isolation system, sufficient to achieve a user-specified TPG. (The process is documented in a) a topical report, funded by the US Department of Energy, and submitted to the US Nuclear Regulatory Commission for review and possible endorsement, and b) an MCEER report.) The process includes the development of a seismic fragility function and a seismic displacement demand curve for the isolation system. This paper lays out the risk calculation process presented in Yu *et al.* (2023) and provides sufficient data for engineers to recover the outcomes presented here. The process is parsed into steps and demonstrated using sample isolation systems and seismic site used in Yu *et al.* (2023). A MATLAB code for the risk calculation is provided.

NOTATIONS

β	The logarithmic standard deviation of a seismic fragility curve; a composite quantity considering the variabilities in isolation-system demand and/or capacity
D_{50}	The median of a seismic fragility curve, namely, isolation-system displacement at a probability of unacceptable performance of 50%; median displacement capacity of an isolation system
ΔE	Mean annual frequency of occurrence; width of a shaking level on an isolation-system displacement demand curve
MAFE	Mean annual frequency of exceedance, namely, the reciprocal of the return period; vertical axis of a seismic hazard curve or an isolation-system displacement demand curve
p_f	Probability of unacceptable performance of an isolation system; vertical axis of a seismic fragility curve
R	Seismic risk
TPG	Target performance goal, denoted P_f in ASCE 4-16 (2017) and ASCE 43-19 (2021)

BASE-ISOLATED REACTOR BUILDING

Introduction

An advanced nuclear reactor building with a mass of 8920 tonnes, including the basemat and internal equipment, is used to demonstrate the risk calculation. A seismic isolation system is installed below the basemat and above the foundation. The required performance of the isolation system is the unrestricted horizontal displacement sufficient to achieve a target performance goal, TPG. Details are provided in Yu *et al*. (2023).

An oscillator model of the base-isolated reactor building, with degrees of freedom in the two horizontal directions, is built for response-history analysis in SAP2000 (CSI 2020). The analysis is performed for two-component horizontal input motions. The numerical model is sufficient to compute horizontal isolation-system displacements (e.g., Mosqueda *et al.* 2004).

Isolation systems

Three 2D horizontal, 2-second isolation systems are implemented beneath the reactor building to illustrate the risk-calculation process: 1) linear isolators (e.g., elastomeric, natural rubber bearings), 2) linear isolators with supplemental nonlinear fluid viscous dampers (FVDs), and 3) bilinear isolators (e.g., spherical sliding bearings). Other systems are considered in Yu *et al*. (2023) but not reported here.

Table 1 presents the mechanical properties of the three isolation systems in the horizontal directions. (Vertical properties are not reported because vertical input shaking and responses are not considered, as noted above.) Figure 1 presents the horizontal force-displacement (*F*-*u*) relationship for the isolation systems and the dampers. The *F*-*u* relationship for system 1, shown in Figure 1a, is viscoelastic, which is defined by a horizontal isolation stiffness, k_{iso}, and a viscous damping ratio. Given that the isolation period is 2 seconds and the superstructure mass is 8,920 tonnes, $k_{iso} = 8.8 \times 10^4$ kN/m. Assuming 5% of critical damping in the elastomer, the damping coefficient c_{iso} is 2.8×10^3 kN-s/m. System 2 is composed of the linear isolators of system 1 and nonlinear FVDs in the two horizontal directions. Eight identical dampers are assumed for system 2: four along each horizontal axis of the building. Figure 1b presents the *F*-*u* relationship for the nonlinear FVDs, defined by a damping coefficient, c_d, and a velocity exponent, δ, less than 1. Herein, δ is 0.3 and c_d is 5000 kN-(s/m)$^{0.3}$ along each horizontal axis of the building ($c_{d,i} = 1250$ kN-(s/m)$^{0.3}$ for each damper). The aggregated *F*-*u* relationship for system 2 is the sum of those shown in Figure 1a (linear system) and Figure 1b (nonlinear dampers). System 3 exhibits the bilinear hysteresis of Figure 1c. The system is composed of single concave spherical sliding isolators. The *F-u* relationship is characterized by a zero-displacement force intercept Q and a second-slope stiffness, $k_{iso} = 8.8 \times 10^4$ kN/m, for an isolation period of 2 seconds. The first-slope stiffness, k_1, is set to 5.3×10^6 kN/m, which is calculated using Q equal to 6% of the building weight ($= 535$ tonnes) at a displacement d_1 of 1 mm. The period associated with k_1 is 0.26 second. At a displacement d, the effective stiffness, k_{eff}, of the bilinear system is between k_{iso} and k_1.

Table 1: Properties of the three 2D isolation systems for the reactor building, horizontal directions, superstructure mass of 8,920 tonnes, isolation period of 2 seconds

System number	Isolation system	Key properties
1	Linear	$k_{iso} = 8.8 \times 10^4$ kN/m; $c_{iso} = 2.8 \times 10^3$ kN-s/m
2	Linear + nonlinear FVDs	$k_{iso} = 8.8 \times 10^4$ kN/m; $c_{iso} = 2.8 \times 10^3$ kN-s/m; $\delta = 0.3$; $c_d = 5000$ kN-(s/m)$^{0.3}$
3	Bilinear	$k_{iso} = 8.8 \times 10^4$ kN/m; $Q = 535$ tonnes; $k_1 = 5.3 \times 10^6$ kN/m

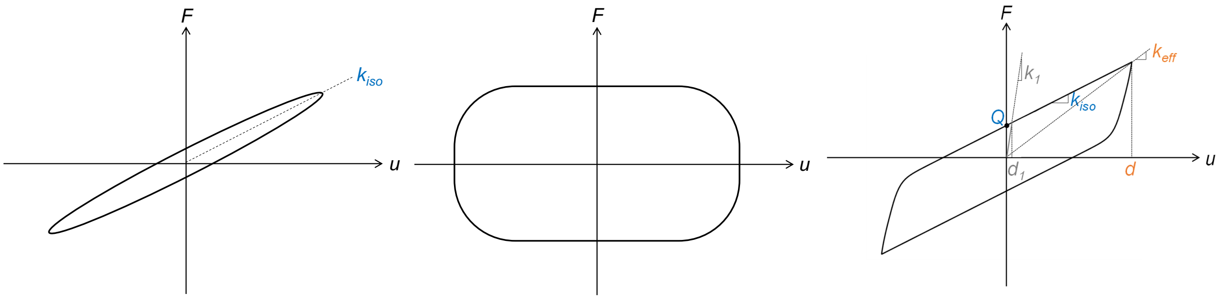

(a) linear (systems 1 and 2) (b) nonlinear FVDs (system 2) (c) bilinear (system 3)

Figure 1. Force-displacement (*F-u*) relationships for the three 2D isolation systems, horizontal directions

Two-degree-of-freedom model

Figure 2 presents the two-degree-of-freedom (2DOF) model: an oscillator composed of a mass and a link element(s) fixed at the ground. This model assumes that the building is rigid, and the dynamic responses are characterized using one mode in each horizontal direction. The total mass of 8920 tonnes, including those of the building, basemat, and equipment, is assigned to the degrees of freedom. The isolation system supporting the building is simulated using the orange link element(s), which accommodates the composite response of the isolators and dampers, if used. The link is placed vertically in the model and has 6 degrees of freedom. The vertical responses are not used. The 3 rotational degrees of freedom are restrained.

The model for systems 1 and 3 uses one link element to simulate the isolation system. The model for system 2 uses two link elements to simulate the isolators and nonlinear FVDs separately. The linear isolators in systems 1 and 2 are modeled using the *linear* link (SAP2000) with the stiffness, k_{iso}, and damping coefficient, c_{iso}, presented in Table 1. The nonlinear FVDs are modeled using the *damper-exponential* link (SAP2000) assigned $\delta_i = 0.3$ and $c_{d,i} = 5000$ kN-(s/m)$^{0.3}$ per Table 1 to provide the aggregated damping along each horizontal axis of the building. System 3 is simulated using the *friction isolator* link (SAP2000) for the bilinear isolators. The parameters, $k_{iso} = 8.8 \times 10^4$ kN/m, $Q = 535$ tonnes, and $k_1 = 5.3 \times 10^6$ kN/m, shown in Table 1 are assigned to the *friction isolator* link.

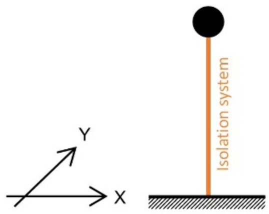

Figure 2. Two-degree-of-freedom (*x* and *y*) model; orange links used to simulate the isolation system

SEISMIC HAZARD AND GROUND MOTION TIME SERIES

To demonstrate the risk calculation process, the reactor building is assumed to be sited in the Central and Eastern United States at the East Tennessee Technology Park (ETTP) in Oak Ridge, Tennessee (TN), near Clinch River. The assumed (latitude, longitude) pair for the site is (35.94°N, 84.40°W). The near-surface soil condition is assumed to be represented by the boundary between site classes C and D (i.e., soft rock and stiff soil) per ASCE/SEI Standard 7-22 (2022).

To enable response-history analysis and risk calculations of the base-isolated reactor building, seismic hazard curves, uniform hazard response spectra (UHRS), and ground motion time series for the Clinch River site are generated using data provided by the U.S. Geological Survey (USGS 2018). Figure 3a presents the seismic hazard curve at the Clinch River site, which relates the mean annual frequency of exceedance (MAFE) and geomean horizontal spectral accelerations at 2 seconds for 5% damping.

Thirty sets of two-component horizontal ground motions are spectrally matched to the 25000-year geomean UHRS (MAFE=4×10^{-5}) using RSPMatch2005 (Hancock *et al.* 2006). Figure 3b presents the UHRS (yellow) and the spectra for the 30 inputs (grey) in the two horizontal directions, for 5% damping. The peak ground acceleration (PGA) is 1 g, and the 2-second spectral acceleration is 0.27 g. The risk calculation considers ground shaking of a range of MAFE. The amplitude of these spectrally matched motions is scaled by a factor of 0.25, 0.5, 0.75, 1, 1.25, 1.5, 2, 3, and 4, and their MAFE are calculated using the 2-second seismic hazard curve. (Yu *et al.* (2023) used different factors to scale ground motions for the risk calculation. For a given isolation system, similar median displacement capacities were determined in Yu *et al.* (2023) and this paper to achieve the same TPG.) Table 2 presents the 2-second spectral accelerations (Sa) and MAFE for the 9 scale factors. The 9 pairs of (Sa, MAFE) are identified using blue circles shown in Figure 3a. Response-history analysis is performed for the 9 shaking intensities. (The use of ground motions spectrally matched to the UHRS at MAFE=4×10^{-5} and the scale factors derived from the 2-second hazard curve implies that the same spectral shape is used for all 9 MAFE. This is a simplification.)

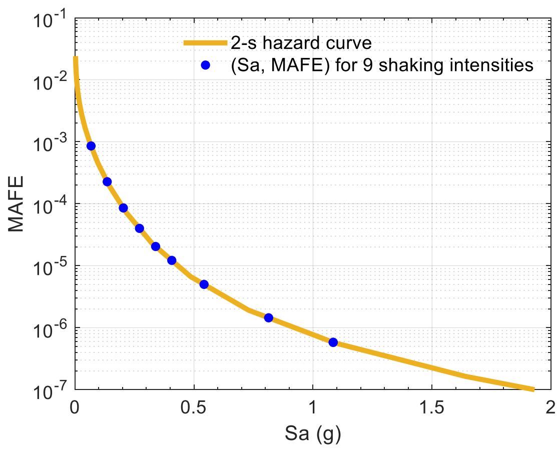

(a) 2-second seismic hazard curve

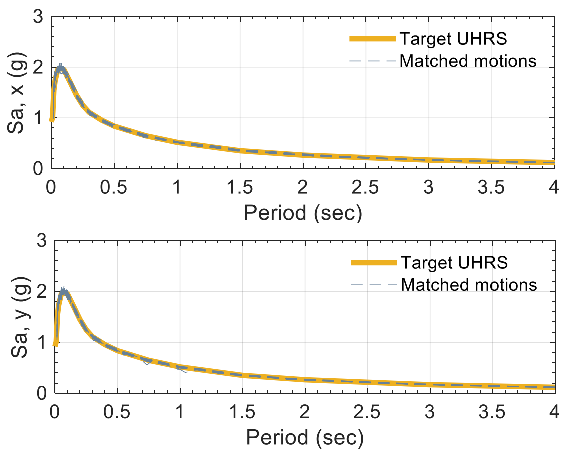

(b) 25,000-year UHRS and spectrally matched motions, PGA=1 g

Figure 3. Seismic hazard data, geomean horizontal, 5% damping, Clinch River, CD soil

Table 2: Data for the 9 shaking levels, (Sa, MAFE) pairs on the 2-second seismic hazard curve

Shaking level	Scale factor	Sa (g)	MAFE
1	0.25	0.07	8.55E-04
2	0.5	0.14	2.26E-04
3	0.75	0.20	8.54E-05
4	1	0.27	4.00E-05
5	1.25	0.34	2.04E-05
6	1.5	0.41	1.22E-05
7	2	0.54	4.99E-06
8	3	0.81	1.44E-06
9	4	1.08	5.80E-07

ACHIEVING A RISK TARGET FOR A SEISMIC ISOLATION SYSTEM

Introduction

A risk-informed process is presented to establish the required median displacement capacity of an isolation system, sufficient to achieve a target performance goal (TPG). Figure 4 illustrates the process, including the development of a seismic fragility function and a seismic displacement demand curve for the isolation system. The displacement demand curve relates the MAFE and the mean maximum horizontal displacement of the isolation system, generated using data from response-history analysis. The isolation-system fragility function is defined by a median displacement capacity and a logarithmic standard deviation. The fragility function is integrated over the displacement demand curve to compute the seismic risk, namely, the mean annual frequency (MAF) of an unacceptable performance of the isolation system. The median displacement capacity of the isolation system is determined by incrementing the median of the fragility curve until the computed risk is equal to or smaller than the TPG. The median displacement capacity is confirmed by prototype testing, noting that such testing will provide a lower bound on capacity, and perhaps by a very significant margin. The process is demonstrated below for the three isolation systems.

Displacement demand curves

Yu *et al.* (2023) provides two approaches for developing displacement demand curves, which lead to similar seismic risks for a given seismic fragility function. The simpler approach is presented here.

The two-degree-of-freedom model is analyzed for the 9 levels of shaking, for each ground motion in a set of 30, for each isolation system. Displacements at the degree of freedom in the two horizontal directions (x and y) are extracted. The square root of the sum of the squares (SRSS) is used to calculate the peak horizontal isolation-system displacement for a given input motion, by combining x- and y-directional components at each time step. The mean of the 30 peak horizontal displacements is computed for each shaking level and isolation system; results are presented in Table 3. Figure 5a presents the displacement demand curve for each isolation system, generated using the MAFE and peak displacements reported in Table 3. (Note that the authors are not advocating for considerations of ground shaking at return periods not supported by data, per shaking level 5, 6, 7, 8, and 9 in Table 3, but rather are illustrating a process.)

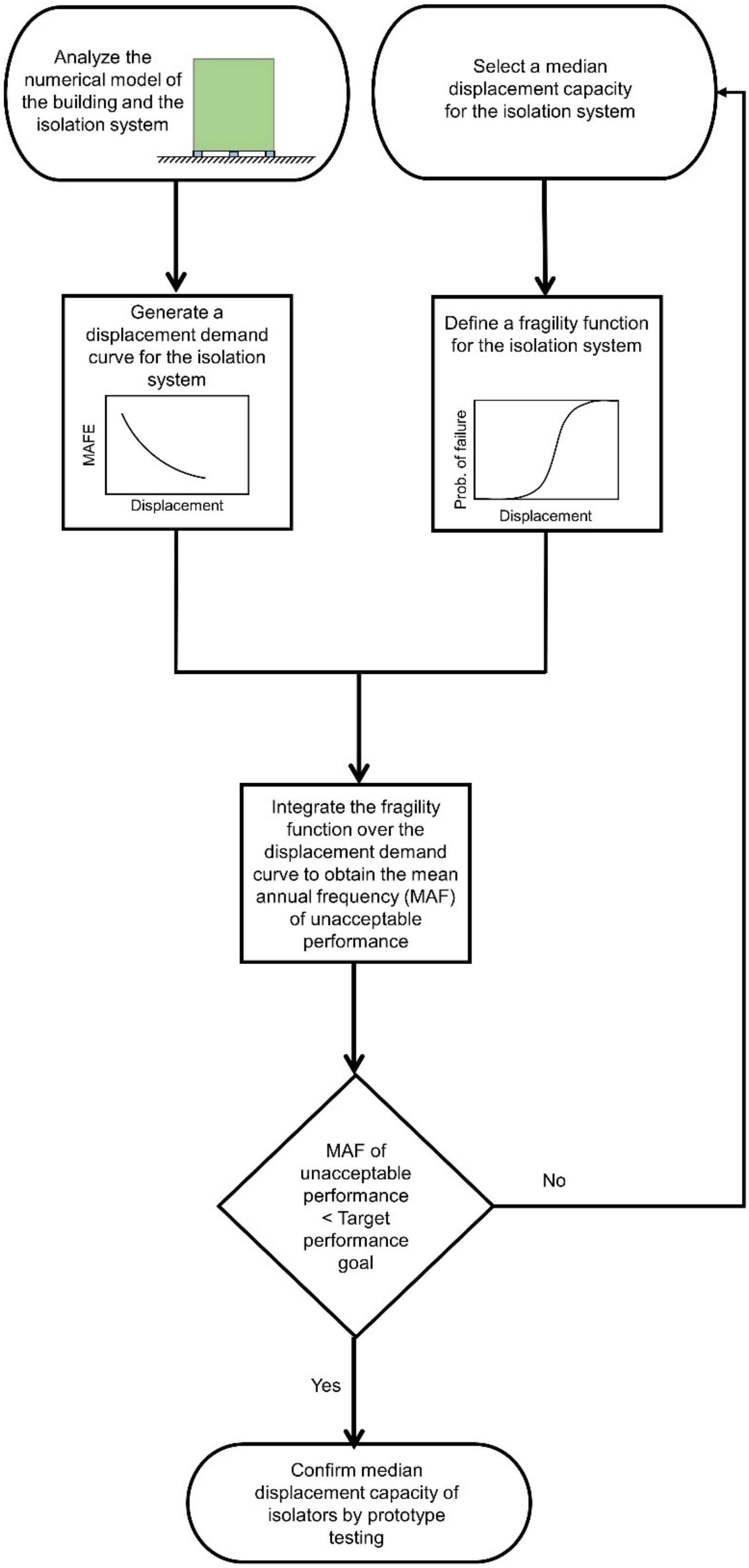

Figure 4. Workflow to achieving a target performance goal for an isolation system (Yu *et al.* 2023)

Table 3: Information used to generate isolation-system displacement demand curves

		Peak horizontal displacement (mm)		
Shaking intensity	MAFE	System 1	System 2	System 3
1	8.55E-04	76	26	15
2	2.26E-04	153	71	58
3	8.54E-05	229	125	118
4	4.00E-05	305	183	189
5	2.04E-05	381	243	266
6	1.22E-05	458	305	348
7	4.99E-06	610	434	527
8	1.44E-06	916	699	912
9	5.80E-07	1221	972	1317

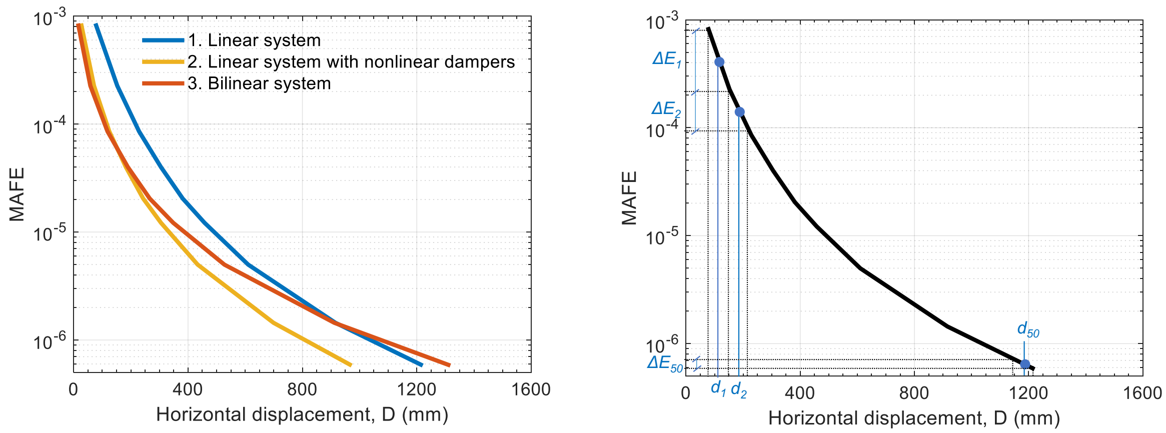

(a) three isolation systems (b) discretization, system 1

Figure 5. Displacement demand curves generated using data from Table 3, Clinch River, CD soil

Seismic fragility functions

Figure 6 presents a sample fragility function. The fragility function relates the isolation-system displacement and the probability of unacceptable performance (p_f) described as a cumulative log-normal distribution defined by a median displacement capacity, D_{50}, and a logarithmic standard deviation, β. The median and the logarithmic standard deviation are assumed to be independent per standard US nuclear practice.

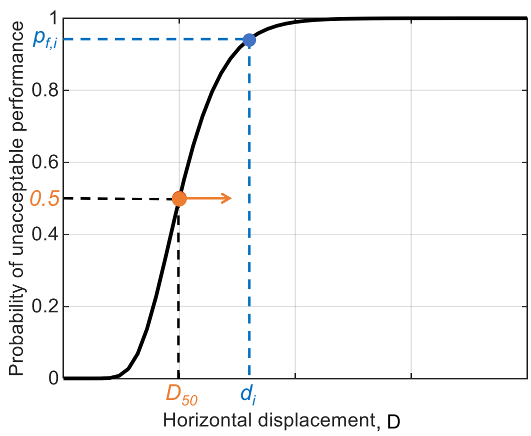

Figure 6. Generic seismic fragility curve of an isolation system, median, D_{50}, adjusted until achieving the target performance goal

The logarithmic standard deviation, β, for the seismic fragility function is a composite quantity considering the variability in ground motions (β_{gm}), the mechanical properties of the isolation system (β_i), and the distribution of mass in the isolated superstructure (β_m):

$$\beta = \sqrt{\beta_{gm}^2 + \beta_i^2 + \beta_m^2} \quad (1)$$

Yu *et al.* (2023) established values of β for linear and nonlinear isolation systems of 0.20 and 0.30 respectively. A value of 0.3 for β is used here for the 3 isolation systems to illustrate the risk calculation process.

Risk calculation

The fragility function is integrated over the displacement demand curve, resulting in seismic risk, namely, MAF of unacceptable performance of an isolation system. To enable the integration, the displacement demand curve is discretized into a number (n) of increments of horizontal displacement, namely, d_i for i = 1 to n. Fifty increments are used here, namely, d_i for i = 1 to 50 noted in Figure 5. The mean annual frequency for each increment, ΔE_i, can be extracted from Figure 5. The probability of unacceptable performance of the isolation system, $p_{f,i}$, at d_i can be extracted from the fragility function, noted as blue in Figure 6. The seismic risk, R, is calculated as:

$$R = \sum_{i=1}^{50} \Delta E_i \times p_{f,i} \quad (2)$$

Increasing the median displacement capacity, D_{50}, reduces the seismic risk, R. The value for D_{50}, noted as orange in Figure 6, is increased until the computed risk is equal to or smaller than the target performance goal, namely, $R \le \text{TPG}$.

Table 4 presents the required median displacement capacities, D_{50}, for each of the isolation systems to achieve TPGs of 1×10^{-4} (1/10000 years), 4×10^{-5} (1/25000 years), and 2×10^{-5} (1/50000 years). Figure 7 presents fragility functions generated using data from Table 4, with D_{50} noted using black solid circles. For a given TPG, the required median displacement capacities for the three isolation systems vary: see Figure 7a for the fragility functions for TPG $=1\times10^{-4}$. For a given system, the greater the median displacement capacity, the more stringent (lower) the TPG: see Figure 7b for the fragility functions of system 1 for the three TPGs. (All the listed D_{50} are substantially smaller than the displacement capacities of elastomeric and sliding isolators, and 1D nonlinear fluid viscous dampers, installed in mission-critical buildings in the US in regions of high seismic hazard.)

Table 4: Required median displacement capacities, D_{50}, to achieve different target performance goals (TPGs), Clinch River, CD soil, $\beta=0.3$

		TPG = 1×10^{-4}	TPG = 4×10^{-5}	TPG = 2×10^{-5}
Isolation system		D_{50} (mm)		
1	Linear	240	340	435
2	Linear + nonlinear FVDs	125	198	270
3	Bilinear	114	202	292

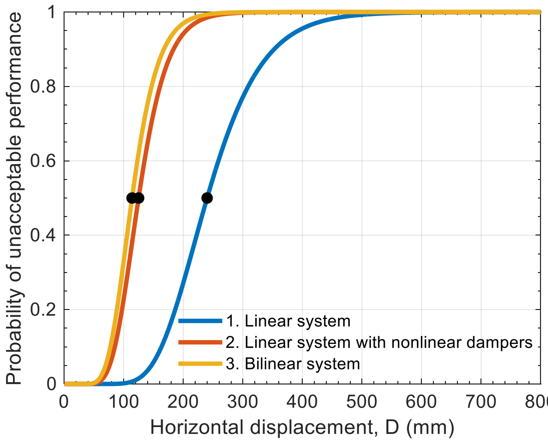

(a) 3 isolation systems, TPG=1×10^{-4}

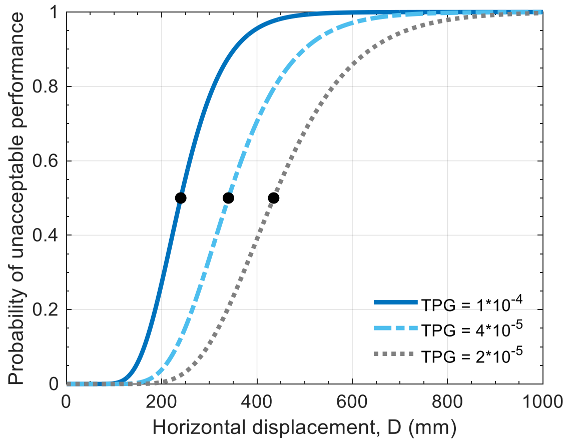

(b) system 1, three TPGs

Figure 7. Fragility functions of the isolation systems with median capacities D_{50} that achieve the target performance goals (TPGs)

SUMMARY AND CONCLUSIONS

Yu *et al.* (2023) provides a risk-based process to establish the median displacement capacity of an isolation system, sufficient to achieve a user-specified target performance goal (TPG). The process includes the development of a seismic fragility function and a seismic displacement demand curve for a user-specified isolation system. The fragility function is integrated over the displacement demand curve to compute the seismic risk. The median displacement capacity of the isolation system is determined by incrementing the median of the fragility curve until the computed risk is equal to or less than the TPG. The median capacity of the isolation system is confirmed by prototype testing per ASCE/SEI 4-16 and 43-19, as augmented by Yu *et al.* (2023).

This paper demonstrates the process using three horizontal isolation systems for an advanced nuclear reactor at Clinch River, TN. Sufficient data and a MATLAB code for risk calculation is provided to enable others to reproduce the outcomes presented here. Required median displacement capacities for the three isolation systems, at the Clinch River site, are calculated for TPGs = 1×10^{-4}, 4×10^{-5}, and 2×10^{-5}. All required median displacements are substantially smaller than the displacement capacities of the considered isolation systems installed in mission-critical buildings in the US in regions of high seismic hazard, namely, a significant margin is provided.

APPENDIX: MATLAB CODE FOR THE RISK CALCULATIONS

A MATLAB code for the risk calculations for system 1 and a target performance goal of 1×10^{-4} is provided below.

```
%% Risk calculation for system 1
D = [76, 153, 229, 305, 381, 458, 610, 916, 1221]; % Mean peak displacement of the isolation system
MAFE = [8.545E-04, 2.262E-04, 8.542E-05, 4.000E-05, 2.041E-05, 1.218E-05, 4.989E-06, 1.443E-06, 5.797E-07]; % Mean annual frequency of exceedance (MAFE) at each D
Num = 50; % Number of increments of displacement for discretization
D_b = linspace(D(1), D(end), Num+1); % Upper and lower bounds of displacement represented by di
d_i = 0.5*(D_b(1:end-1)+D_b(2:end)); % Increments of displacement, di
MAFE_b = 10.^(interp1(D, log10(MAFE), D_b)); % Upper and lower bounds of MAFE represented by di
d_E = MAFE_b(1:end-1)-MAFE_b(2:end); % Frequency of occurrence, ΔEi, for each di

TPG = 10^(-4); % Target performance goal
beta = 0.3; % Logarithmic standard deviation for the fragility curve
```

```
# Iterations for determining the median displacement capacity to achieve the TPG
C = 0;
while 1
    D_50 = D(1)*(1+C/100); % Median displacement capacity of the isolation system, increasing 1% for each loop
    p_f = logncdf(d_i, log(D_50), beta); % Calculate probability of unacceptable performance of the isolation system with a displacement at di
    Risk = sum(p_f.*d_E); % Risk; fragility function integrated over the demand curve
    if Risk < TPG
        break
    end
    C=C+1;
end

figure (1) % Plot displacement demand curve
semilogy(D, MAFE)
xlabel('Horizontal displacement, D (mm)'); ylabel('MAFE');
set(gca,'fontsize',13,'fontname','Arial','XMinorTick','on','YMinorTick','on')

figure (2) % Plot fragility function
x=1:1:800; % Provide a displacement range
p = logncdf(x, log(D_50), beta); % Calculate probability of unacceptable performance
plot(x,p)
xlabel('Horizontal displacement, D (mm)'); ylabel('Probability of unacceptable performance');
set(gca,'fontsize',13,'fontname','Arial','XMinorTick','on','YMinorTick','on')
```

ACKNOWLEDGMENTS

The information, data, and work presented herein were funded in part by the U.S. Department of Energy, under Award Number DE-NE0008932. The views and opinions of the authors expressed herein do not necessarily state or reflect those of the United States Government, the Idaho National Laboratory, Southern Company, and Kairos Power. The authors thank Dr. Faizan Ul Haq Mir of the University at Buffalo and Dr. Mohamed Talaat of Simpson, Gumpertz & Heger for their input to and review of the risk calculation procedure.

REFERENCES

American Society of Civil Engineers (ASCE) (2017). "Seismic analysis of safety-related nuclear structures and commentary." *ASCE/SEI 4-16*, ASCE, Reston, VA.

American Society of Civil Engineers (ASCE) (2021). "Seismic design criteria for structures, systems, and components in nuclear facilities." *ASCE/SEI 43-19*, ASCE, Reston, VA.

American Society of Civil Engineers (ASCE) (2022). "Minimum design loads and associated criteria for buildings and other structures." *ASCE/SEI 7-22*, ASCE, Reston, VA.

Hancock, J., Watson-Lamprey, J., Abrahamson, N. A., Bommer, J. J., Markatis, A., McCoyh, E., and Mendis, R. (2006). "An improved method of matching response spectra of recorded earthquake ground motion using wavelets." *Journal of Earthquake Engineering*, 10(spec01), 67-89.

Mosqueda, G., Whittaker, A. S., and Fenves, G. L. (2004). "Characterization and modeling of friction pendulum bearings subjected to multiple components of excitation." *Journal of Structural Engineering*, 130(3), 433-442.

United States Geological Survey (USGS) (2018). "Hazard curves for the 2018 update of the U.S. National Seismic Hazard Model." <https://www.sciencebase.gov/catalog/item/5d559795e4b01d82ce8e3fef>. (Feb, 2021).

Yu, C.-C., Mir, F. U. H., Carmichael, B. M., Chisholm, B. M., Redd, J., Bolisetti, C., and Whittaker, A. S. (2023). "Guidelines for implementing seismic base isolation in advanced nuclear reactors." *MCEER-23-0003*, University at Buffalo, Buffalo, NY.